Published in final edited form as:
J Manipulative Physiol Ther. 2012 ; 35(9): 669–677. doi:10.1016/j.jmpt.2012.10.010.

Optimized Prediction of Contact Force Application During Side-Lying Lumbar Manipulation

Casey A. Myers, MSc[a], **Brian A. Enebo, DC, PhD**[b], and **Bradley S. Davidson, PhD**[c]

[a]Graduate Research Assistant, Mechanical and Materials Engineering, University of Denver, Denver, CO.

[b]Associate Clinical Professor and Chiropractor, Integrative Medicine Program at University of Colorado Hospital, Division of General Internal Medicine, University of Colorado Denver School of Medicine, Aurora, CO.

[c]Assistant Professor, Mechanical and Materials Engineering, University of Denver, Denver, CO.

Abstract

Objectives—The purposes of this study included the following: (1) to predict L3 contact force during side-lying lumbar manipulation by combining direct and indirect measurements into a single mathematical framework and (2) to assess the accuracy and confidence of predicting L3 contact force using common least squares (CLS) and weighted least squares (WLS) methods.

Methods—Five participants with no history of lumbar pain underwent 10 high-velocity, low-amplitude lumbar spinal manipulations at L3 in a side-lying position. Data from 5 low-force criterion standard trials where the L3 contact force was directly measured were used to generate participant-specific force prediction algorithms. These algorithms were used to predict L3 contact force in 5 experimental trials performed at therapeutic levels. The accuracy and effectiveness of CLS and WLS methods were compared.

Results—Differences between the CLS-predicted forces and the criterion standard–measured forces were 621.0 ± 193.5 N. Differences between the WLS-predicted forces and the criterion standard–measured forces were −3.6 ± 9.1 N. The 95% limits of agreement ranged from 234.0 to 1008.0 N for the CLS and −21.9 to 14.7 N for the WLS. During both the criterion standard and experimental trials, the CLS overestimated contact forces with larger variance than the WLS.

Conclusion—This novel method to predict spinal contact force combines direct and indirect measurements into a single framework and preserves clinically relevant practitioner-participant contacts. As advanced instrumentation becomes available, this framework will enable advancements in training and high-quality research on mechanisms of spinal manipulative therapy.

Keywords

Manipulation; Spinal; Lumbar vertebrae; Biomechanics

Accurate and reliable measurement of contact forces applied during spinal manipulative therapy (SMT) is an important aspect to research, education, patient safety, and clinical application. Competent delivery of SMT requires the practitioner to be adept at modulating

Submit requests for reprints to: Bradley S. Davidson, PhD, 2390 S York St, Denver, CO 80208 (Bradley.Davidson@du.edu). .

Potential Conflicts of Interest No conflicts of interest were reported for this study.

peak contact force and rate of force application.[1-5] However, standards for clinical effectiveness and patient safety currently do not exist for manipulative force application. In addition, few opportunities exist for practitioners and students to receive quantitative feedback on SMT delivery.

Several methods exist to measure in vivo contact forces during SMT[3,4,6-12] and can be classified into 2 categories: direct measurement and indirect measurement. Direct force measurement is often implemented using pressure mats or load cells placed between the practitioner and the patient.[8,11-13] An advantage of direct measurement is that forces are measured at the site of contact. However, pressure mats can only measure forces oriented perpendicular to the contact surface, and shear forces are not considered. This method is commonly used to assess SMT with the participant lying prone on the treatment table, and care is taken to deliver a force perpendicular to the surface.[8,11,13-15] As a result, direct measurement has limited application in high-velocity, low-amplitude (HVLA) manipulations of the cervical and lumbar spine because shear and rotational forces are present.

Indirect force measurement is accomplished by applying an inverse dynamics paradigm with resultant forces recorded from a force platform embedded in the treatment table.[4,9,16] An advantage of this method is that the practitioner maintains clinically realistic contact with the participant at the site of the manipulation. However, this method ignores energy loss that occurs between the force application points and the measurement site. In addition, this method can only be used when there is a single contact point between the practitioner and the patient. For example, Triano and Schultz[4] isolated the thrust force during side-lying lumbar spine manipulation by creating structures specifically designed to eliminate the effect of stabilizing forces from other contacts to the force platform.

When analyzing manual procedures such as side-lying SMT, direct and indirect measurement techniques will likely yield conflicting results of contact force magnitude and direction. Therefore, one approach to improve contact force measurement is to combine the 2 methods into a single framework while preserving the advantages of each. Combining these experimental methods will capture more measurements than required and will result in an overdetermined mathematical system. Instead of being a limitation, this feature is beneficial when any measurements are unreliable, less reliable than other measurements, or unavailable. Mathematicians and engineers have developed a wide array of tools to solve overdetermined systems.[17] Common least squares (CLS) and weighted least squares (WLS) are 2 attractive options that preserve the mathematical structure and measurement dependencies inherent when combining direct and indirect force measurements of SMT. Common least squares uses a pseudoinversion of a rectangular matrix, and WLS performs the same fundamental calculation while systematically emphasizing or deemphasizing the contribution of each measurement according to the reliability of the measurement. Weighted least squares has been successfully implemented in other biomechanical applications such as estimating 2-dimensional joint torques during quiet stance[18] and 3-dimensional joint torques during overground walking.[19]

The objectives of this investigation were (1) to combine direct and indirect force measurements during a side-lying manipulation into a single mathematical framework and (2) to assess the accuracy and confidence of predicting L3 contact force using CLS and WLS methods. We hypothesized that WLS would produce lower error when compared with a CLS approach and that the framework and resulting measurement weights can be efficiently used to predict contact force when a therapeutic level of SMT is applied.

Methods

Data Collection

Five participants (3 men: age, 34 ± 6.1 years; height, 180.3 ± 2.6 cm; mass, 83.6 ± 8.3 kg; 2 women: age, 25 ± 3.5 years; height, 171.4 ± 1.8 cm; mass, 59.1 ± 1.3 kg) provided informed consent to participate in this investigation. Each participant had no history of lumbar pain or injury and underwent 10 HVLA lumbar spinal manipulations at L3 in a right side-lying position.

To best preserve the traditional mechanics of a side-lying manipulation, multiple points of contact between the practitioner and the participant were allowed. Although structures designed to isolate forces applied by the practitioner[4] were not used, practitioner-participant contact was limited to 3 locations: (1) practitioner left hand with participant left shoulder, (2) practitioner right thigh with lateral aspect of participant left thigh, and (3) practitioner right hand with participant left L3 mammillary process (Fig 1). A manipulation was discarded if the practitioner contacted the participant at an additional location during the thrust (eg, practitioner's chest contacted the participant).

The first 5 HVLA manipulations served as criterion standard trials. These manipulations were performed with a load cell in the right hand of the practitioner, which directly measured L3 contact forces. The surface area of the load cell was approximately 1 in^2 and interacted with the vertebra similar to hypothenar contact when no load cell was used in the experimental trials. During the criterion standard trials, the practitioner used a contact force that was lower than normal therapeutic load to minimize discomfort caused by the load cell. The criterion standard trials combined direct measurement of the L3 contact force with a set of data that included direct measurement of thigh and shoulder contact force, indirect force measurement, and motion capture data to generate a prediction algorithm for L3 contact force (described in "Contact Force Prediction"). The last 5 HVLA manipulations served as experimental trials. The load cell at the L3 contact point was removed for these manipulations, and they were performed with normal therapeutic contact and loading. All other measurements in the data set were collected in the same way as the criterion standard trials. Data sets from the experimental trials were used to demonstrate the effectiveness of the contact force prediction algorithms established during the criterion standard trials.

Direct Force Measurement—Force magnitudes at the participant contacts (left shoulder, thigh, and L3) were recorded using uniaxial load cells placed between the participant and the practitioner (Cooper Instruments, Warrenton, VA). The load cells were securely fixed to the practitioner using elastic straps. Aquaplast splinting material (Qfix, Avondale, PA) placed over the skin of the participant was used to form a rigid contact surface at the thigh and shoulder (Fig 1).

Indirect Force Measurement—Resultant forces and moments from all contacts were measured with a force platform (Bertec Corporation, Columbus, OH) embedded in a standard treatment table (Physical Enterprise, Petaluma, CA). The modified treatment table consisted of 3 isolated sections: head, body, and foot (Fig 2). The force platform was embedded only in the body section.

During each manipulation, the participant was supported primarily by the body section and, as little weight possible, was placed on the head and foot sections. Therefore, the 3 contact forces applied to the participant were absorbed by force platform instead of the other supporting sections of the table.

Contact force direction and practitioner kinematics were measured using an infrared motion capture system (Vicon, Centennial, CO). Reflective markers were placed on the practitioner and load cells during a calibration collection. After calibration, load cell markers were removed and reconstructed as virtual markers during each manipulation. *Direction of the force* was defined by a vector perpendicular to the contact surface of the load cell.

Load cell and force platform data were sampled at 2000 Hz and conditioned with a low-pass Butterworth filter (zero-phase lag, 20-Hz cutoff). These data were downsampled to 100 Hz for synchronization with motion capture data. Average time delay between load cell application and force platform measurement was approximately 20 milliseconds for each participant. Therefore, an equivalent offset was applied between the 2 signals for algorithm development.

Contact Force Prediction

L3 contact force applied to the participant during the 5 experimental trials was predicted using an algorithmic model built from the 5 criterion standard trials. The model combined direct measurements from load cells and motion capture with the indirect measurement of resultant forces and moments from the force platform to form a linear set of overdetermined equations. This was solved in an optimization routine to predict the L3 contact force vector (Fig 3).

The 3 components of the spine contact force ($F_x^{(sp)}, F_y^{(sp)}, F_z^{(sp)}$) with respect to a global coordinate system (x, y, z) can be estimated using 3 independent methods. Each method relies on a different combination of the force, moment, and kinematic measurements: force balancing, moment balancing, and direction-constrained force balancing.

Force Balancing—The force balancing method combines direct contact force data from the load cells at the shoulder and thigh contacts with indirect resultant force data from the force platform. Because orientation of each force is known with respect to the global coordinate system, the spine contact forces are calculated as follows:

$$\begin{aligned} F_x^{(sp)} &= F_x^{(fp)} - F_x^{(sh)}\Big) - F_x^{(th)} \\ F_y^{(sp)} &= F_y^{(fp)} - F_y^{(sh)} - F_y^{(th)} \\ F_z^{(sp)} &= F_z^{(fp)} - F_z^{(sh)} - F_z^{(th)} \end{aligned} \quad (1)$$

where $F_x^{(fp)}, F_y^{(fp)}$„ and $F_z^{(fp)}$, are resultant force vectors recorded from the force platform; $F_x^{(sh)}, F_y^{(sh)}$, and $F_z^{(sh)}$ are force vectors calculated at the shoulder contact; and $F_x^{(th)}, F_y^{(th)}$, and $F_z^{(th)}$ are force vectors calculated at the thigh contact.

Moment Balancing—The moment balancing method combines moments calculated using force data from the load cells at the shoulder and thigh contacts and distance from fixed coordinate system axes with indirect resultant moment data from the force platform:

$$\begin{bmatrix} 0 & d_z^{(sp)} & d_y^{(sp)} \\ d_z^{(sp)} & 0 & d_x^{(sp)} \\ d_y^{(sp)} & d_x^{(sp)} & 0 \end{bmatrix} \begin{Bmatrix} F_x^{(sp)} \\ F_y^{(sp)} \\ F_z^{(sp)} \end{Bmatrix} = \begin{Bmatrix} M_x^{(fp)} - F_z^{(sh)} d_y^{(sh)} - F_y^{(sh)} d_z^{(sh)} - F_z^{(th)} d_y^{(th)} - F_y^{(th)} d_z^{(th)} \\ M_y^{(fp)} - F_z^{(sh)} d_x^{(sh)} - F_x^{(sh)} d_z^{(sh)} - F_z^{(th)} d_x^{(th)} - F_x^{(th)} d_z^{(th)} \\ M_z^{(fp)} - F_y^{(sh)} d_x^{(sh)} - F_x^{(sh)} d_y^{(sh)} - F_y^{(th)} d_x^{(th)} - F_x^{(th)} d_y^{(th)} \end{Bmatrix} \quad (2)$$

where $M_x^{(fp)}$, $M_y^{(fp)}$, and $M_z^{(fp)}$ are resultant moments recorded from the force platform at the force platform origin; $d_x^{(sp)}$, $d_y^{(sp)}$, and $F_z^{(sp)}$ define orthogonal distances from the force platform origin to the L3 spinal contact; $d_x^{(sh)}$, $d_y^{(sh)}$, and $d_z^{(sh)}$ define orthogonal distances from the force platform origin to the shoulder contact; and $d_x^{(th)}$, $d_y^{(th)}$, and $d_z^{(th)}$ define orthogonal distances from the force platform origin to the thigh contact.

Direction-Constrained Force Balancing—The direction-constrained force balancing method provides an additional constraint to the force balancing method. The scalar magnitude of the spinal contact force is calculated using the same data as Eq. 1:

$$F_{est}^{(sp)} = \sqrt{\left(F_x^{(fp)} - F_x^{(sh)} - F_x^{(th)}\right)^2 + \left(F_y^{(fp)} - F_y^{(sh)} - F_y^{(th)}\right)^2 + \left(F_z^{(fp)} - F_z^{(sh)} - F_z^{(th)}\right)^2} \quad (3)$$

and is reoriented to coincide with the line of thrust, which is assumed to be delivered in line with the practitioner forearm:

$$\begin{aligned} F_x^{(sp)} &= F_{est}^{(sp)} u_x^{(fa)} \\ F_y^{(sp)} &= F_{est}^{(sp)} u_y^{(fa)} \\ F_z^{(sp)} &= F_{est}^{(sp)} u_z^{(fa)} \end{aligned} \quad (4)$$

where $u_x^{(fa)}$, $u_y^{(fa)}$, and $u_z^{(fa)}$ define the direction cosines of the forearm:

$$\begin{aligned} u_x^{(fa)} &= \frac{l_x^{(fa)}}{\sqrt{l_x^{(fa)2} + l_y^{(fa)2} + l_z^{(fa)2}}}, \\ u_y^{(fa)} &= \frac{l_y^{(fa)}}{\sqrt{l_x^{(fa)2} + l_y^{(fa)2} + l_z^{(fa)2}}}, \\ u_z^{(fa)} &= \frac{l_z^{(fa)}}{\sqrt{l_x^{(fa)2} + l_y^{(fa)2} + l_z^{(fa)2}}} \end{aligned} \quad (5)$$

and $l_x^{(fa)}$, $l_y^{(fa)}$, and $l_z^{(fa)}$ are scalar projections of the practitioner forearm onto the global axes.

By combining Eqs. 1 to 3 into a single system, an overdetermined mathematical representation is formed, which has more equations than unknowns. Although each of the 3 methods can be used to solve for the L3 contact force, a significant limitation in each is the rigid-body assumption. Because neither the practitioner nor the participant behaves as rigid bodies, errors that are not captured in Eqs. 1 to 3 exist in the experimental measurement and an error term must be included. The resulting system takes the matrix form $A \cdot F^{(sp)} = b + e$:

(6)

where $e_x^{(\cdot)}$, $e_y^{(\cdot)}$, and $e_z^{(\cdot)}$ represent the error associated with each row calculation in the global coordinate system.

The system was solved using 2 approaches: CLS and WLS. The CLS procedure predicts the spine contact forces by left-multiplying b by A^+, which is the 3 × 9 pseudoinverse of A:

$$F_{\text{pred}}^{(\text{sp})} = A^+ \cdot b \quad (7)$$

where $F_{\text{pred}}^{(\text{sp})}$ represents the components of the predicted L3 contact force $F_x^{(\text{sp})}$, $F_y^{(\text{sp})}$, $F_z^{(\text{sp})}$.

Although the CLS is valid for an overdetermined system and creates some robustness in the solution, it cannot be tuned to account for systematic error.

The WLS procedure accounts for systematic error by weighting the contribution of each calculation using the following form:

$$\begin{aligned} \text{minimize } f \quad & \left(F_{\text{pred}}^{(\text{sp})}, W\right) \\ & = \left[\left(A \cdot F_{\text{pred}}^{(\text{sp})} = b\right)^T W \left(A \cdot F_{\text{pred}}^{(\text{sp})} = b\right)\right] \end{aligned} \quad (8)$$

where W is a 9 × 9 weighting matrix of scalars only in the diagonal elements. These scalars emphasize or deemphasize the contribution of the individual rows in Eq. 6 to the spinal contact force calculation.

A participant-specific W was determined through an optimization procedure using the 5 sets of criterion standard data. A nonlinear downhill simplex was used to evaluate the objective function:

$$\text{minimize } f\left(F_{\text{pred}}^{(\text{sp})}\right) = \Sigma\left(|F_{\text{meas}}^{(\text{sp})}| - \left|F_{\text{pred}}^{(\text{sp})}\right|\right)^2 \quad (9)$$

where $|F_{\text{meas}}^{(\text{sp})}|$ is the magnitude of the measured L3 spinal contact force collected during the criterion standard trials and $|F_{\text{pred}}^{(\text{sp})}|$ is the magnitude of the predicted L3 spinal contact force. A total of 2400 iterations were used to determine W. Convergence was confirmed when changes in the objective function fell below 0.01.

Data Analysis

A 5-fold cross-validation technique was used on the criterion standard trials from each participant to create the participant-specific weighting matrix used to predict L3 contact force. To accomplish the 5-fold method, 50 milliseconds surrounding the peak force in 4 of the 5 criterion standard trials were simultaneously optimized using Eqs. 8 and 9. The resulting W was used to predict the L3 contact force on the remaining criterion standard trial for validation.[17] This process (4 criterion standard then 1 validation) was repeated for every possible combination of the 5 criterion standard trials (Fig 4). The W matrix that produced the smallest error between predicted force and measured force was used to predict L3 contact force for the participant in the experimental trials (therapeutic load, contact force unknown/not directly measured with load cell) using Eq. 8.

Predicted contact forces using CLS and WLS were compared with the validation measurement to evaluate the error of each approach. Bland-Altman plots were generated for visual comparison, and 95% limits of agreement were calculated (mean difference ± 2 SDs).

Peak forces were compared across contact points (left shoulder, thigh, and L3) using a 1-way repeated-measures analysis of variance, followed by pairwise comparisons using Tukey Honestly Significant Difference test. Peak forces at the L3 contact were compared across criterion standard and experimental trials using a paired t test. Level of significance was set at $\alpha = .05$ for all statistical tests.

Results

The mean absolute difference between the CLS-predicted force and the measured force was 621.0 ± 193.5 N. The mean absolute difference between the WLS-predicted force and the measured force was −3.6 ± 9.1 N. The 95% limits of agreement, or the range in which 95% of the prediction errors occurred, were 234.0 to 1008.0 N for the CLS and −21.9 to 14.7 N for the WLS.

During both the criterion standard and experimental trials, the CLS overestimated contact forces with larger variance than the WLS (Fig 5).

Estimated peak force at L3 during the experimental trials was 88.4 ± 26.0 N greater than the peak force measured during the criterion standard trials for all 5 participants. In addition, within-participant variability was smaller for the peak force delivered during the experimental trials (Table 1).

Significant analysis of variance ($P = .009$) indicated differences in peak forces across contact points. Pairwise comparisons demonstrated that peak force at L3 was greater than peak force applied at the left shoulder, but with no differences between peak forces at L3 and the thigh and between shoulder and thigh. Significant t test ($P < .001$) indicated that predicted peak forces at L3 during experimental trials were greater than predicted peak forces at L3 during criterion standard trials (Fig 6).

Discussion

Direct and indirect methods of contact force measurement were combined into a single mathematical framework. Using this framework, the accuracy and confidence of predicting L3 contact force using a CLS approach and WLS approach were assessed during side-lying manipulation. Spinal contact forces produced during side-lying spinal manipulation predicted using a WLS approach produced lower error when compared with a CLS approach. In addition, the WLS approach was successfully used to predict the L3 contact force during manipulation that closely matched what would be performed in a clinical setting.

Combining direct and indirect measurements introduces a novel framework to predict contact forces during SMT while preserving clinically relevant contact between practitioner and participant. For example, contact points at the shoulder and thigh, which remove tissue slack and stabilize the patient, have not been incorporated into force measurement during SMT. This approach also accounts for the unique style of each practitioner by incorporating practitioner kinematics at the contact site into the force estimation.

Key characteristics of HVLA spinal manipulation (preload force and high rate of force application during thrust)[9,15] were present when using the WLS approach, whereas the CLS approach did not demonstrate clear patterns containing these characteristics. A peak contact

force of 337.2 ± 66.9 N during the experimental trials was slightly lower than previous indirect measurement[4] but falls within previously reported range (300-500 N) of using direct measurement.[15]

The WLS approach of force prediction may provide a better understanding of how all SMT contact forces contribute to patient outcomes during a complex therapy. It is common for the practitioner to stabilize the patient with one hand, thrust with the other hand, and exert a rotational torque with their body weight through their lower extremity. However, force magnitude and direction at these contact points have not been reported. An average peak force of 180.8 ± 52.9 N was delivered at the shoulder, 267.3 ± 48.5 N at the thigh, and 337.2 ± 66.9 N at the L3 spinal level. This is an interesting outcome considering that the thigh contact force is not different in magnitude than the L3 contact force, but the longer lever arm results in a much greater rotational moment about the spine. The therapeutic effects of these differences warrant further investigation.

Manual therapy students may benefit from the data produced using this method as they learn and refine their practice of SMT. Peak force, peak moment, preload force, time to peak force, and rate of force production are all measures that have been used to assess changes in SMT performance.[20-24] However, this is primarily measured using instrumented mannequins[20-22,25] or, in cases when human participants are used, with qualitative verbal and visual feedback.[26] The method developed in this investigation provides multiple sources of quantitative feedback on force application while maintaining relevant clinical contact. In addition to helping train students to produce consistent force application, interacting with these data may also increase understanding of SMT biomechanics and ultimately lead to better treatment planning and application of SMT.

Limitations

The purpose of this investigation was to provide a proof of concept for novel spinal manipulative force prediction, and several limitations currently prevent deployment of this framework in settings outside a research laboratory. First, instrumenting the practitioner with load cells may alter the force application when compared with a normal clinic environment. Future study could reduce this limitation through alternate methods of force instrumentation that provides more direct contact with the participant. Second, the magnitude of the force delivered during the criterion standard trials and used to develop the predictive algorithm was lower than the force applied during the experimental trials. Lower force application was necessary to minimize potential patient discomfort that would occur if large therapeutic loads were applied through the contact surface of the load cell. Therefore, prediction error is possible at the higher force levels applied in the experimental trials. However, training the algorithm on a wide range of forces (average variability of 45.1 N) in the criterion standard trials helps to minimize prediction error at these larger forces. Third, the motion capture hardware used to measure practitioner kinematics may be both cost and space prohibitive. Although the encumbrances in each of these factors are steadily declining with technological advances, these items are unavailable in many research and education settings. Last, this framework was developed and tested only on HVLA manipulation in a side-lying position. As measurement hardware becomes more accessible and these methods undergo further refinement, these limitations will be reduced, making combined measurement available in settings outside the research laboratory.

Future Studies

Future investigations will examine the general application of this framework to other SMT methods and treatment locations. In addition, the relationship between force application and clinical outcomes can be better established with accurate measurement of spinal

manipulative forces. We anticipate that combining these force estimation methods with assessment of muscle activity and pain in patients with and without low back pain will lead to a better understanding of the underlining mechanisms of SMT.

Conclusion

In summary, we present a novel method to predict spinal contact force that combines direct and indirect measurements into a single framework that preserves clinically relevant contact points. The WLS approach produced an acceptably low error when predicting the force applied during a side-lying manipulation. With further advances in instrumentation and computational refinement, we anticipate that this method will enable advanced training methods and high-quality research on mechanisms of SMT.

Acknowledgments

The authors thank Andrea Wanamaker for her assistance in designing and fabricating the instrumentation necessary to perform this investigation.

Funding Sources This project was supported by Award No. R00AT004983-03 (to B.S.D.) from the National Institutes of Health (National Center for Complementary and Alternative Medicine). The content is solely the responsibility of the authors and does not necessarily represent the official views of the NCCAM or the National Institutes of Health.

REFERENCES

1. Downie AS, Vemulpad S, Bull PW. Quantifying the high-velocity, low-amplitude spinal manipulative thrust: a systematic review. J Manipulative Physiol Ther. 2010; 33:542–53. [PubMed: 20937432]
2. Enebo B, Sherwood D. Experience and practice organization in learning a simulated high-velocity low-amplitude task. Manipulative Physiol Ther. 2005; 28:33–43.
3. Hessell B, Herzog W, Conway P, McEwen M. Experimental measurement of the force exerted during spinal manipulation using the Thompson technique. J Manipulative Physiol Ther. 1990; 13:448–53. [PubMed: 2146356]
4. Triano J, Schultz A. Loads transmitted during lumbosacral spinal manipulative therapy. Spine. 1997; 22:1955–64. [PubMed: 9306523]
5. Triano JJ, Gissler T, Forgie M, Milwid D. Maturation in rate of high-velocity, low-amplitude force development. J Manipulative Physiol Ther. 2011; 34:173–80. [PubMed: 21492752]
6. Colloca CJ, Cunliffe C, Pinnock MH, Kim Y-K, Hinrichs RN. Force-time profile characterization of the McTimoney toggletorque-recoil technique. J Manipulative Physiol Ther. 2009; 32:372–8. [PubMed: 19539120]
7. Snodgrass SJ, Rivett Da, Robertson VJ, Stojanovski E. Forces applied to the cervical spine during posteroanterior mobilization. J Manipulative Physiol Ther. 2009; 32:72–83. [PubMed: 19121465]
8. Perle SM, Kawchuk GN. Pressures generated during spinal manipulation and their association with hand anatomy. J Manipulative Physiol Ther. 2005; 28:e1–7. [PubMed: 15883571]
9. Triano JJ. Biomechanics of spinal manipulative therapy. Spine J. 2001; 1:121–30. [PubMed: 14588392]
10. Tsung BYS, Evans J, Tong P, Lee RYW. Measurement of lumbar spine loads and motions during rotational mobilization. J Manipulative Physiol Ther. 2005; 28:238–44. [PubMed: 15883576]
11. Herzog W, Kats M, Symons B. The effective forces transmitted by high-speed, low-amplitude thoracic manipulation. Spine. 2001; 26:2105–11. [PubMed: 11698887]
12. Forand D, Drover J, Suleman Z, Symons B, Herzog W. The forces applied by female and male chiropractors during thoracic spinal manipulation. J Manipulative Physiol Ther. 2004; 27:49–56. [PubMed: 14739874]
13. Herzog W, Kats M, Symons B. The effective forces transmitted by high-speed, low-amplitude thoracic manipulation. Spine. 2001; 26:2105–10. [discussion 2110-1]. [PubMed: 11698887]

14. Herzog W. Forces exerted during spinal manipulative therapy. Spine. 1993; 18:1206–12. [PubMed: 8362328]
15. Herzog, W. The mechanical, neuromuscular, and physiological effects produced by spinal manipulation. Churchill Livingstone; Philadelphia: 2000.
16. Cambridge EDJ, Triano JJ, Ross JK, Abbott MS. Comparison of force development strategies of spinal manipulation used for thoracic pain. Man Ther. 2012; 17:241–5. [PubMed: 22386279]
17. Nelles, O. Nonlinear system identification. Springer; Berlin: 2001.
18. Kuoa D. A least-squares estimation approach to improving the precision of inverse dynamics computations. J Biomech Eng. 1998; 120:148–59. [PubMed: 9675694]
19. van den Bogert AJ, Su A. A weighted least squares method for inverse dynamic analysis. Comput Methods Biomech. 2008; 11:3–9.
20. Descarreaux M, Dugas C. Learning spinal manipulation skills: assessment of biomechanical parameters in a 5-year longitudinal study. J Manipulative Physiol Ther. 2010; 33:226–30. [PubMed: 20350677]
21. Descarreaux M, Dugas C, Lalanne K, Vincelette M, Normand MC. Learning spinal manipulation: the importance of augmented feedback relating to various kinetic parameters. Spine J. 2006; 6:138–45. [PubMed: 16517384]
22. Descarreaux M, Dugas C, Raymond J, Normand MC. Kinetic analysis of expertise in spinal manipulative therapy using an instrumented manikin. J Chiropr Med. 2005; 4:53–60. [PubMed: 19674647]
23. Cohen E, Triano JJ, McGregor M, Papakyriakou M. Biomechanical performance of spinal manipulation therapy by newly trained vs. practicing providers: does experience transfer to unfamiliar procedures? J Manipulative Physiol Ther. 1995; 18:347–52. [PubMed: 7595108]
24. van Zoest GGJM, van den Berg HTCM, Holtkamp FC. Three-dimensionality of contact forces during clinical manual examination and treatment: a new measuring system. Clin Biomech. 2002; 17:719–22.
25. Stemper BD, Hallman JJ, Peterson BM. An experimental study of chest compression during chiropractic manipulation of the thoracic spine using an anthropomorphic test device. J Manipulative Physiol Ther. 2011; 34:290–6. [PubMed: 21640252]
26. Triano JJ, Scaringe J, Bougie J, Rogers C. Effects of visual feedback on manipulation performance and patient ratings. J Manipulative Physiol Ther. 2006; 29:378–85. [PubMed: 16762666]

Practical Applications

- By combining direct and indirect force measurements into an optimized framework, multiple sources of information on force application are used while maintaining relevant clinical contact.
- These methods can be used to train clinicians and students to produce consistent force application.
- Interacting with these data may also increase understanding of SMT biomechanics, and ultimately leading to better treatment planning and application of SMT.

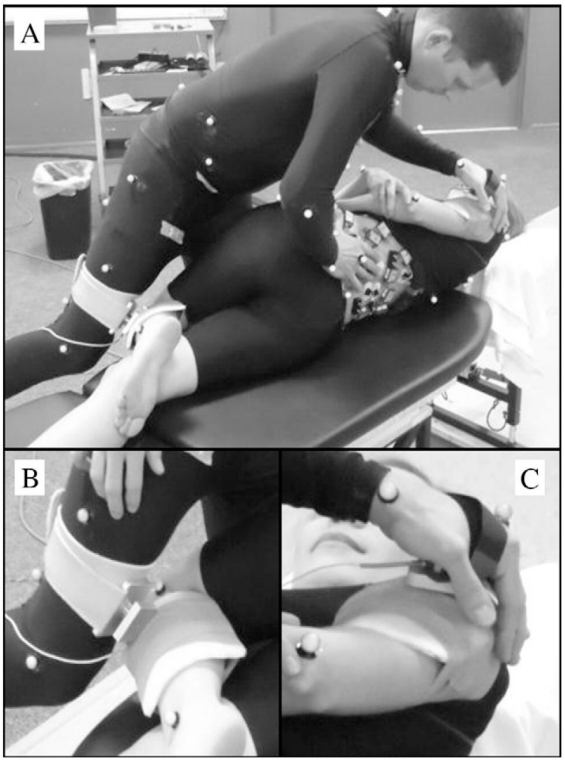

Fig 1.

A, Practitioner and participant positions during the side-lying manipulation showing contact at the thigh, left shoulder, and L3 spinal level. B, Enlarged view of the thigh contact. C, Enlarged view of the shoulder contact.

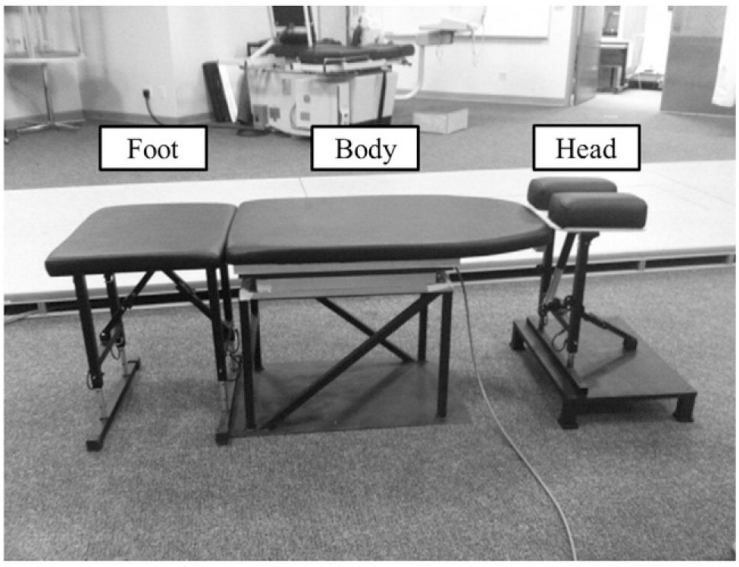

Fig 2.
Modified treatment table with embedded force platform in the body section. Note that the head, body, and foot sections are not connected.

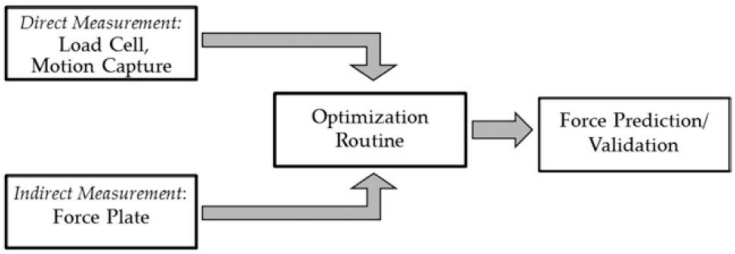

Fig 3.
Schematic of the data flow taken to predict spinal contact force.

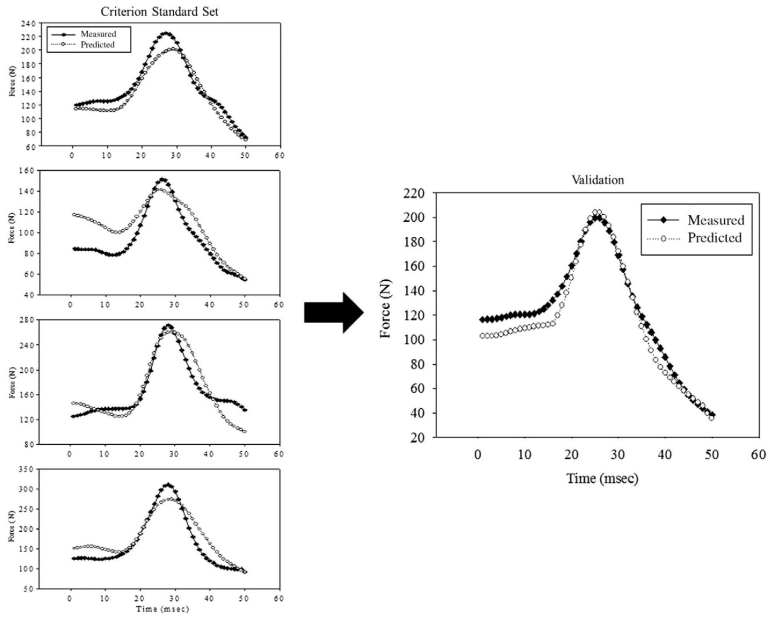

Fig 4.

Measured L3 force (◆) and predicted L3 force (○) from 1 participant showing 1 iteration of the k-fold cross-validation procedure. The weighting matrix, W, was optimized to minimize predictive error of L3 force in 4 criterion standard manipulations. L3 force from a fifth criterion standard manipulation was used to validate the optimized W by comparing the predicted force with the measured force. This was repeated 5 times for each participant, and the W with the smallest error was used to predict L3 force in the experimental trials.

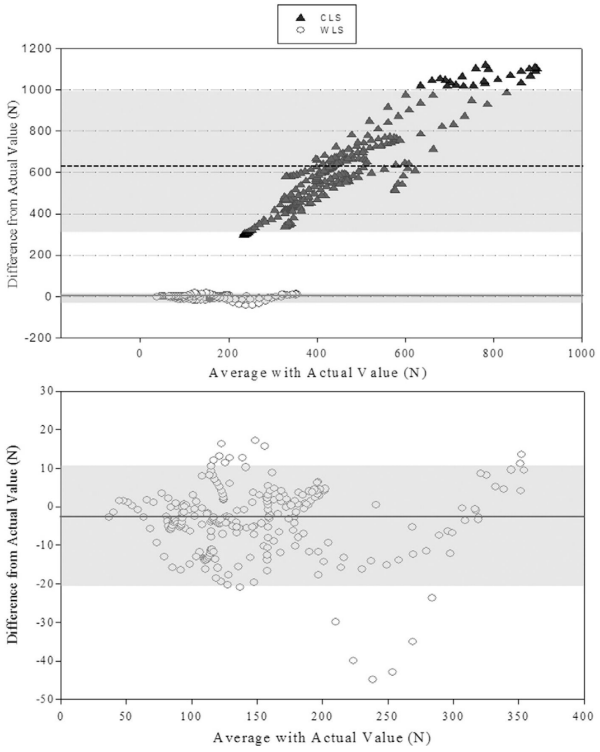

Fig 5.

Bland-Altman plot of the CLS (▲) force prediction and the WLS (○) force prediction (top panel) and enlarged Bland-Altman plot for the WLS force prediction only (bottom panel). This plot illustrates the average value of the measured force and the predicted force on the horizontal axis and the difference of the predicted force and the measured force on the vertical axis (prediction error). The dashed line shows the average prediction error of the CLS, and the solid line shows the average error of the WLS. Shaded regions represent the 95% limits of agreement for the 2 methods.

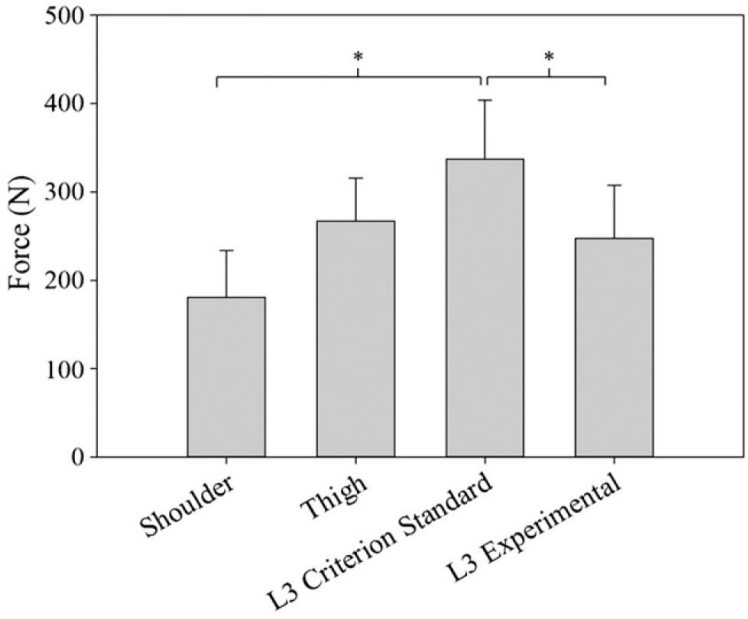

Fig 6.

Average peak force magnitudes and SD measured at the 3 contact points during the experimental trials. The L3 contact force was compared between the experimental and criterion standard trials. *Significant difference.

Mathematical Nomenclature

$F_x^{(sp)}, F_y^{(sp)}, F_z^{(sp)}$	force vector components at L3 spine contact
$F_x^{(fp)}, F_y^{(fp)}, F_z^{(fp)}$	force vector components measured by force platform
$F_x^{(sh)}, F_y^{(sh)}, F_z^{(sh)}$	force vector components at shoulder contact
$F_x^{(th)}, F_y^{(th)}, F_z^{(th)}$	force vector components at thigh contact
$M_x^{(fp)}, M_y^{(fp)}, M_z^{(fp)}$	resultant moments from force platform about force platform axes
$d_x^{(sp)}, d_y^{(sp)}, d_z^{(sp)}$	orthogonal distances from force platform origin to the L3 spinal contact
$d_x^{(sh)}, d_y^{(sh)}, d_z^{(sh)}$	orthogonal distances from force platform origin to the shoulder contact
$d_x^{(th)}, d_y^{(th)}, d_z^{(th)}$	orthogonal distances from force platform origin to the thigh contact
$F_{pred}^{(sp)}$	spinal contact force estimated from force balancing
$u_x^{(fa)}, u_y^{(fa)}, u_z^{(fa)}$	direction cosines of the forearm
$l_x^{(fa)}, l_y^{(fa)}, l_z^{(fa)}$	scalar projections of the forearm onto the *x, y*, and *z* axes
$e_x^{(\cdot)}, e_y^{(\cdot)}, e_z^{(\cdot)}$	error associated with each calculation in the respective coordinate directions
$F_{pred}^{(sp)}$	predicted components of the L3 contact force $F_x^{(sp)}, F_y^{(sp)}, F_z^{(sp)}$
WPRED	9 × 9 diagonal weighting matrix
$\lvert F_{pred}^{(sp)} \rvert$	predicted force magnitude at L3 spinal contact
$\lvert F_{meas}^{(sp)} \rvert$	measured force magnitude at L3 spinal contact

Table 1

Average peak force magnitudes (SD) measured at the force platform and the 3 contact points during experimental trials at a therapeutic load

	Participant 1	Participant 2	Participant 3	Participant 4	Participant 5
Force platform	881.2 (109.0)	1057.9 (94.9)	1286.6 (62.5)	1070.0 (137.7)	959.3 (89.4)
Shoulder contact	114.4 (22.5)	164.1 (9.4)	166.0 (25.7)	256.6 (21.8)	202.9 (33.9)
Thigh contact	269.9 (23.6)	204.8 (20.0)	256.9 (38.4)	306.4 (51.7)	298.8 (29.0)
L3 contact	326.6 (53.3)	273.2 (12.8)	296.7 (21.6)	441.7 (37.4)	347.6 (30.2)
L3 crierion standard (N)	215.2 (53.4)	219.2 (40.3)	215.1 (36.4)	323.9 (48.1)	269.9 (48.8)

The L3 peak force magnitudes measured during the criterion standard trials are highlighted in gray.